Spectral Information Adjustment Using Unsharp Masking and Bayesian Classifier for Automatic Building Extraction from Urban Satellite Imagery

Seyed Mostafa Mirhassani[1], Bardia Yousefi[1], Alireza Moghaddamjoo[2]

[1]Department of Electrical and Robotic Engineering, Shahrood University of Technology, Shahrood, IRAN
[2]Department of Electrical Engineering, Amirkabir University of Technology, Tehran, IRAN
bardia.yousefi@ieee.org

Abstract: Building extraction in remote sensing images of urban areas is based on various classification techniques, demands development of various image processing and pattern recognition algorithms. Current techniques have poor performances in low local contrast conditions and require preprocessing methods for improving local contrast. In this novel approach, Unsharp Masking [USM] and Motion based Unsharp Masking [MUSM] methods are introduced to increase the local contrast in class images. In the proposed classification techniques, wherever spatial relationships drawn from buildings are imperative, the structural pattern recognition is properly utilized. In very high resolution remote sensing images where, the Bayesian classifier performs recognition of very small building and other cluttered areas, USM techniques are essential in amplifying the high frequency components of the original image which is used for building discrimination. The novelty of this paper is performing preprocessing technique which modifies frequency components of satellite image. In order to benchmark the algorithm, some of the Google Earth three bands (RGB) images were used. It is comprehend able from the results that the accuracy of small and large building classification using unsharp masking technique increases as compared with the methods without any preprocessing steps.
[Seyed Mostafa Mirhassani, Bardia Yousefi, Alireza Moghaddamjoo. Automatic Building Extraction from Urban Satellite Imagery Using Bayesian Classifier and Unsharp Masking as Spectral Information. Journal of American Science 2012;8(1):554-564]. (ISSN: 1545-1003). **http://www.americanscience.org**. 77

Keywords: Building Extraction; Classification of Urban Areas; Motion Based Unsharp Masking [MUSM]; Unsharp Masking [USM]; Bayesian Classifier

1. Introduction

Remote sensing imagery makes the monitoring of the earth's surface and atmosphere possible in various scales. As the technology of the imagery sensors improves, higher quality remote sensing images become readily available. Recently, some efforts have been developed for sending new small satellites to provide hyper spectral satellite images as well as analysis of the acquired hyper spectral data. Training remote sensing specialists, to collect helpful information from the existing data, is a cumbersome work. However, automatic processes have been paid more attention in scientific communities. Due to advent new generations of microprocessors, more complex image processing tasks are viable. As an instant, automatic classification of remote sensing images of urban areas provides beneficial information for traffic surveillance, earth survey, map updating, GIS [3] urban planning, emergency response, management, and security applications. Therefore, automated and semiautomatic methods for the classification of roads, buildings, and other land cover types in the urban areas are of much interest.

Classification of man-made objects is realized using pixel-based or object-based methods. Pixel-based methods [6, 4, 17, 18, 13] include construction of an n-dimensional pattern vectors from the gray level data of each part of input image and classification of these vectors. In this case, the reference vectors are obtained during training phase based on the bank of remote sensing image database. In object-based approaches, instead of individual pixels, groups of pixels are considered and processed to be recognized as objects. In this case, neighborhood relationships and shape characteristics are important for classification of such images.

As the resolution of the image increases, the accuracy of the pixel-based methods for classifying multispectral remote sensing imagery decreases. Furthermore, spectral characteristics of different classes might be similar [9]. As a result, discrimination of such classes encounters error. Fuzzy-based methods for classification, confront such problems due to the fuzzy membership of a pixel to different classes [1, 5, 7, 8, 11, 20, 21, 22, 23]. In [8], a fuzzy-based classifier is compared with an artificial neural network (ANN) classifier and proved to be superior in its performance. Fusions of different fuzzy approaches have been utilized in [7] to improve accuracy and fusion of low and high resolution images for changes monitoring. In [15, 5], based on spectral similarity of many urban land cover types and spatial information such as texture and

context, an accurate classification map from input images is developed. Then, a fuzzy classifier is utilized for the classification of urban areas. An object-based method for the classification of dense urban areas from pan-sharpened multispectral IKONOS remote sensing images is introduced in [11]in which, a cascade combination of a fuzzy pixel-based classifier and a fuzzy object-based method has been used. The fuzzy pixel-based classifier extracts the spectral content of the scene while, the fuzzy object-based classifier analyzes the spatial context information. Use of the support vector machine (SVM) to classify urban areas in remote sensing images is presented in [2]. In this approach, the hierarchical relationships between each pixel and the adaptive regions are associated and considered to build the feature vectors. These feature vectors are then applied to an SVM classifier.

In [14, 10], segmentation techniques have been applied to remote sensing imagery for classification. The residuals of morphological opening and closing transforms have been utilized for segmentation [13].

In [19], a technique based on Laplacian operators is introduced. Firstly, Laplacian of the input image is obtained and then a special Bayesian classifier for the classification of buildings is used. In this approach, urban areas, roads and highways are extracted by using size and some of the morphological operations such as opening and closing. In [16] the unsharp masking technique is used as a preprocessing step to improve the local contrast and to intensify the high frequency components of the input image. Then, the developed building classifier in [19] is used for building classification with an improvement of accuracy.

On the other hand, some of the applications of these techniques include: GIS based fire analysis and production of fire-risk Maps [12], GIS urban-information system design and development, GIS in population census [3], Monitoring land use changes in tourism, protection and management of archaeological sites.

In this approach, the USM family image enhancement algorithms including USM and MUSM filtering are employed as preprocessing steps to improve building classification. After image enhancement, image Laplacian and size criterion are used as features to discriminate buildings based on the Bayesian rule. The remainder of this article is organized as follows: In the next section, modified Bayesian classifier is presented and afterwards a motion-based unsharp mask (MUSM) is introduced as an advanced preprocessing tool followed by the experimental results and conclusion.

2. Building Extraction Using Modified Bayesian Discrimination Function

In this section, three preprocessing approaches are considered to be used with Morphological Operations (MO) along with Bayesian discrimination function which includes the base building extractor, (1) USM, (2) MUSM, and (3) Filtered-MUSM methods.

2.1 Building Extraction Strategy

The first stage consists of the extraction of building features from urban images. Image intensity variations give beneficial information from the image objects. Generally, to achieve intensity variations, various filters are proposed in literature. Choosing an appropriate feature for an application is context information dependent. Here, the information of input image intensity variations is obtained from the Laplacian image. One of the most significant superiority of Laplacian among other edge detection methods is its second derivative action as a powerful mean to detect the edges. Furthermore, the edges provided by Laplacian do not need to be thinned because the zero crossings themselves define the edges location. The Laplacian operator is defined as:

$$\nabla^2 I_x(x,y) = \frac{\partial^2 I_x(x,y)}{\partial x^2} + \frac{\partial^2 I_x(x,y)}{\partial y^2} \quad (1)$$

In this approach absolute value of Laplacian is used as a feature for Bayesian rule for building extraction. $P(c_1 \mid \lambda(x,y))$ and $P(c_2 \mid \lambda(x,y))$ are used to represent the probability function associated to the Building Class and None-Building Class, respectively. These densities are estimated and used for multi-Bayesian discrimination rule. the absolute amount of image Laplacian, λ , as the discrimination parameter is set. Hence, $P(c_1 \mid \lambda)$ denotes the probability of Building Class at Laplacian level of λ, irrespective of building size. None-Building Class, denoted by c_2, includes open areas, roads, shadows, and other structures in urban areas. These probability density functions are obtained from Google Earth (Reykjavik, Iceland) remote sensing image database. The boundary of the two classes can be identified by emphasizing on the boundary via following equation:

$$P(c_1 \mid \lambda) \geq P(c_2 \mid \lambda) \quad (2)$$

For $\lambda > 0.5$ Non-boundary pixels of building areas have much lower Laplacian values. Next, small buildings are discriminated from large ones by introducing γ_{SF} , the size discriminating feature, and using the following inequality to perform the classification.

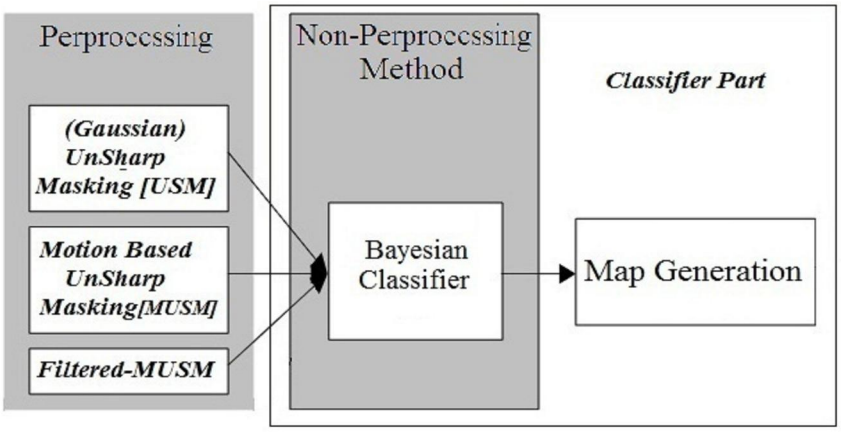

Figure.1. Flowchart of the proposed method

$$P(c_{1S} \mid \gamma_{SF}) \geq P(c_{1L} \mid \gamma_{SF}) \qquad (3)$$

Where c_{1S} and c_{1L} denote "Small" and "Large" building classes respectively. The size discriminating feature, γ_{SF}, and a feature denoted by θ, used to identify indistinguishable regions from non-indistinguishable regions, which will be defined later. Therefore, three features, $\lambda, \gamma_{SF}, \theta$ are used in this classification to identify buildings from non-buildings, large buildings from small buildings, and to discriminate indistinguishable regions from non-indistinguishable regions. It should be noted that indistinguishable regions have a very important role in obtaining three dimensional information of the buildings from their 2D urban images.

2.2 *Applying the USM Method as Pre-Filtering for Building Extraction*

Pixel values of building areas are sometimes close to intensity levels of their surroundings. Additionally, poor contrast in building areas, results in higher classification error. To overcome such problems, unsharp masking is used as a preprocessing step before classification. This operation can improve the local contrast of images and generate more accurate classification results. Therefore, the proposed algorithm consists of two main stages namely, pre-processing stage and classification stage. The unsharp mask filter improves the local image contrast by

$$\tilde{I} = I - a.G.T \qquad (4)$$

In which I and $\tilde{I}$ denote the original image and the unsharp masked image intensities respectively. The blurred image, filtered by a Gaussian mask, is denoted by G. Therefore the three parameters in this formula used to adjust the unsharp mask enhancement; parameter a is used to adjust the edge enhancement level, parameter σ of the Gaussian filter is used to control the level of blurring or averaging in the filtered image, and parameter T is used to control the noise level. Amount of parameter σ, is set equal to one fifth of the size of the Gaussian mask.

Parameter T indicates minimum difference between original image pixels and blurred image pixels before applying the unsharp mask filter.

$$T(x,y) = \begin{cases} 1 & |G(x,y) - I(x,y)| \geq th \\ 0 & o.w. \end{cases} \qquad (5)$$

If, there is no significant change between two images pixels, application of USM filter would add noise to the image. Unsharp masking filter at any direction adds dark and white edges, to improve the local contrast. Consequently, the local contrast is boosted and building edges become more visible.

$$G(x,y) = \sum_{h=-m/2}^{m/2} \sum_{k=-m/2}^{m/2} \frac{1}{2\pi\sigma} e^{-\frac{h^2+k^2}{2\sigma^2}} I(x-h, y-k) \qquad (6)$$

(6) determines $G(x,y)$ which is utilized in (4). (6) Obtains a version of the original image with diminished high frequency components. A Laplacian operator, according to (1), is applied to the unsharp masked image to produce an input image for the Bayesian discriminator. This process makes the image ready for the Bayesian discrimination function. Two classes determined in Bayesian discriminating rule, namely the building class from the non-building, assessing small and large buildings with shadows.

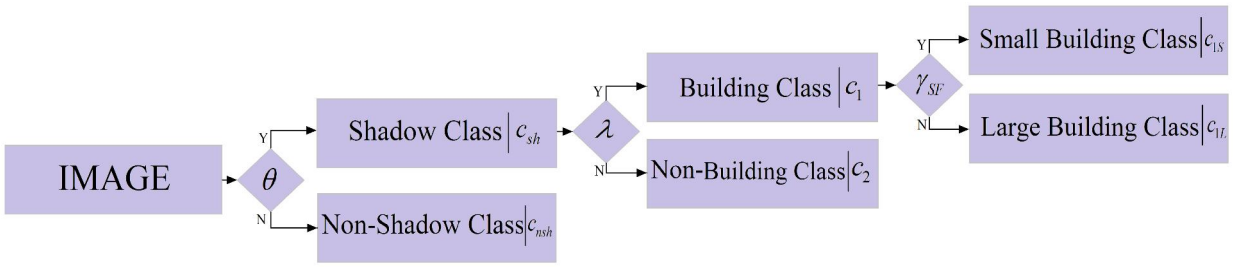

Figure. 2. The horizontal axis is the Laplacian intensity λ and the vertical axis is the probability density function. The upward, middle and downward represent roads, open areas and buildings classes, respectively.

Following classes are classified by Bayesian discrimination rule using same method.

$$I(x,y)=\sum_{s=1}^{n} I(x,y)\cap c_s \qquad s=1,2,...,n \qquad (7)$$

c_s, n denote image classes and the number of whole image. The $I(x,y)$ indicates the whole input image containing $c_1, c_2, \ldots,$ classes of remote sensing images from urban areas.

$$P(I(x,y))=\sum_{s=1}^{n} P(I(x,y)\cap c_s) \qquad (8)$$

Here, n is equal to 2.

$$P(I(x,y))=P(I(x,y)\,|\,c_1)P(c_1)+P(I(x,y)\,|\,c_2)P(c_2) \qquad (9)$$

The shadows are classified using θ feature. It is considerable, that to extract shadows no preprocessing step is utilized. For shadow extraction, θ is image intensity employed as a threshold to be applied on the original image as follows:

$$I(x,y)\le\theta \Rightarrow I(x,y)=SH(x,y) \qquad (10.1)$$

$$\theta\le 0.2 \Rightarrow P(c_{sh}\,|\,\theta)>P(c_{nsh}\,|\,\theta) \qquad (10.2)$$

Where $SH(x,y)$, c_{sh} and c_{nsh} represent shadow image, shadow PDF and non-shadow PDF, respectively.

Figure 3 indicates probability distribution function (PDF) of building, roads and open area classes, when the employed feature is λ. This PDF is obtained by training map in which different classes were manually marked. Considering restrictions of Laplacian between 0 and 1, the following expression could be inferred:

$$0.1\le\lambda\le 0.5 \Rightarrow P(c_1\,|\,\lambda)<P(c_2\,|\,\lambda) \qquad (11)$$

c_1, c_2 represents building and non-building classes attained from discriminating parameter (λ). Secondly, the classifier is operated to assess whether buildings are large or small. Up till this point, γ_{SF} is utilized as a feature, to determine size of buildings. For the second classifier, the following expression is given:

$$150\ge\gamma_{SF} \Rightarrow P(c_{1L}\,|\,\gamma_{SF})>P(c_{1S}\,|\,\gamma_{SF}) \qquad (12)$$

Where c_{1L} and c_{1S} denote Large and small buildings, respectively. As, it is shown in (13), both c_{1L} and c_{1S} are subsets of c_1.

$$\{c_{1L}\bigcup c_{1S}\}\subset c_1 \qquad (13)$$

The mentioned features discriminate the building class, large and small building classes. The mentioned explanations are summarized in Figure 2.

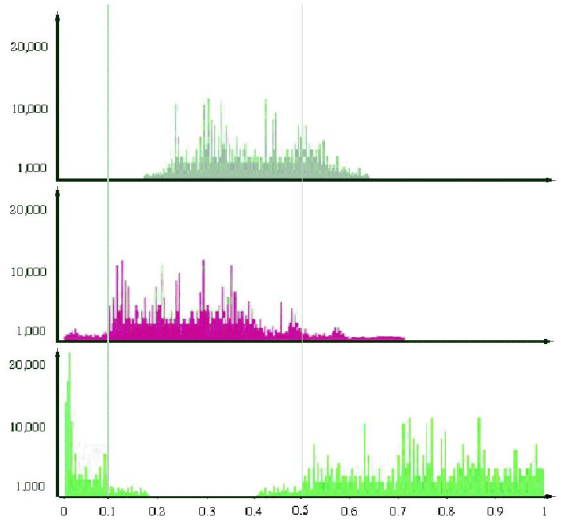

Figure. 3. Summery of classes

2.3 *MUSM Method for Classification of Buildings*

The USM method for the classification of remote sensing images mostly focuses on building extraction. It is inferred from USM results that the building extraction rate multiplies.

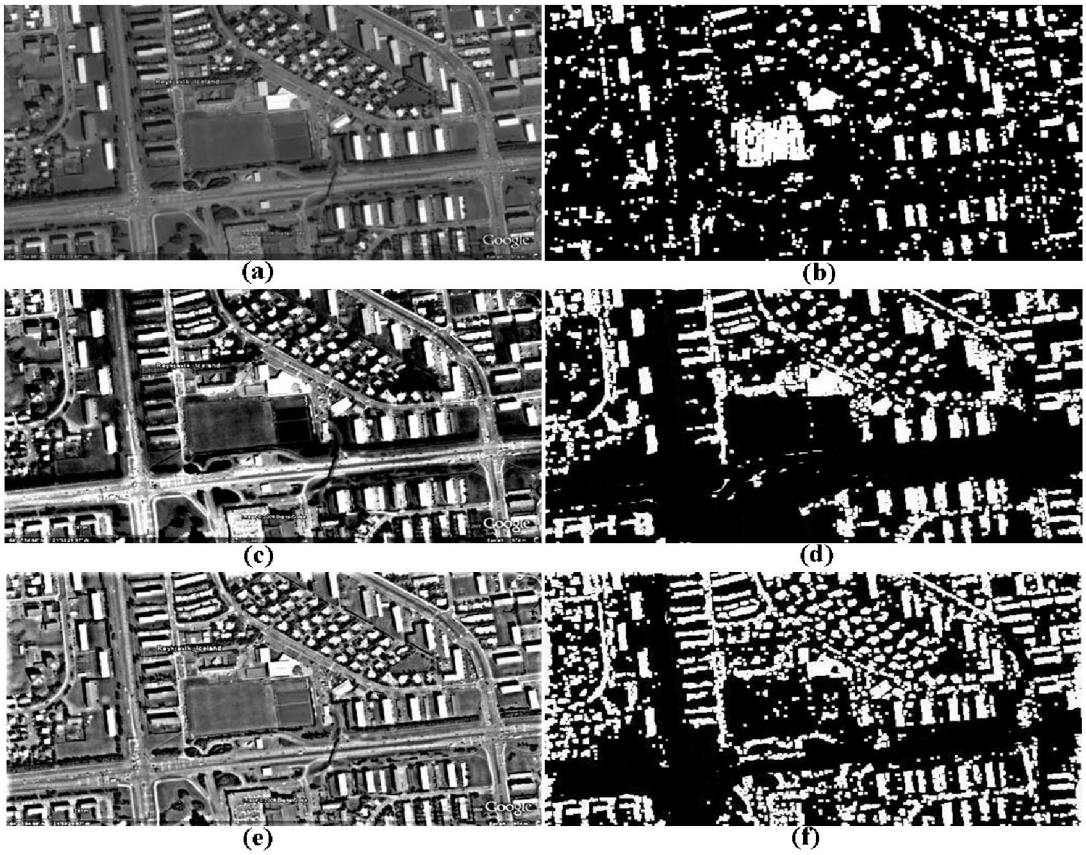

Figure. 4. This figure highlighted some demonstrated results, 4.a original image 4.b Result of none-prefiltering method; 4.c filtered image using USM. 4.d its result. Extraction of small buildings has considerable improvement; 4.e filtered image using MUSM method, 4.f classified version of image using filtered-MUSM method. Experimental results indicate there is enhancement in buildings extracted through this method. However, false positive are reduced due to the elimination of non-building regions in remote sensing using this method.

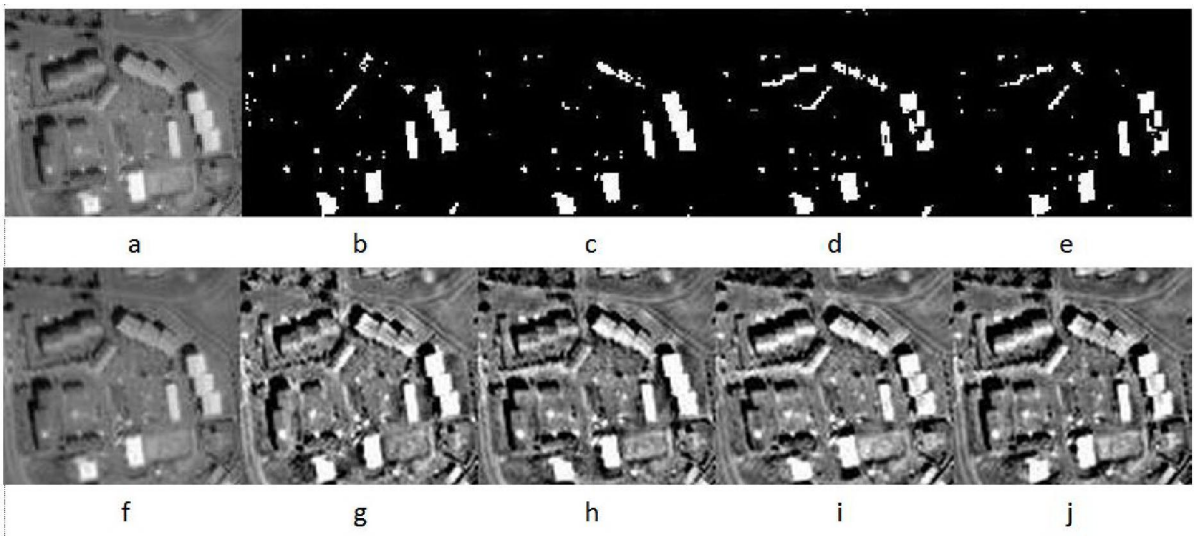

Figure. 5. Effect of applying MUSM filter in different directions on the image. Original image 5.a and 5.d and MUSM filtered images with angles of 0, 45, 90 and 135 degree before 5.g, 5.e, 5.i, 5.j and after 5.b, 5.c, 5.d, 5.e applying threshold. It is obvious that after adjusting the angle of MUSM filter to perpendicular direction of building edges, dark buildings will be detectable too.

As the low frequency image components are eliminated as a result of unsharp masking. The USM method utilizes the Gaussian blurring for matrix G in (4). It can be developed by using a Motion blurring filter in an Unsharp Masking (MUSM). MUSM controls the direction of blurring. It enhances an image sharpening and accordingly building extraction. This section aims to describe the knowledge of image categorization based on modified USM technique. It is different from USM method which employs Gaussian blurring.

In some parts of image, contrast of buildings was weak; consequently they could not be extracted effortlessly. Unsharp Masking has been used in the algorithm as a preprocessing step to improve extraction accuracy in cluttered areas. Unsharp Mask filtering increases the high frequency of the image components. It, however, does not prevent the noise addition unless its threshold parameter, T, is adjusted. Due to applying the MUSM filter, local contrast can be developed in voluntary orientations. The formula of unsharp mask is given in (4). Let I and G be the original image and the blurred image using the Gaussian filter.

a and T are adjusted parameters for the amount of high frequency components and noise reduction factors, respectively. In the MUSM method G denotes motion blurred image instead of Gaussian blurred image. The point spread function (PSF) of motion blurring is given as follows:

$$If\ \ x_o(t) = \frac{A}{T}t \quad and\ y_o(t) = \frac{B}{T}t \tag{14}$$

$$H(u,v) = \frac{T}{\pi(uA+vB)}\sin[\pi(uA+vB)]e^{-j\pi(uA+vB)}$$

Where $\frac{A}{T}$ and $\frac{B}{T}$ denote velocity of motion in horizontal and vertical orientation, correspondingly. x_0 and y_0 denote the number of pixels when the image is elongated. The unsharp mask filter using motion blurred image provides two main advantages. Firstly adding high frequency components lead to noise multiplication to the original image; but the proposed approach reduces the noise in the original image, which is filtered in desired orientations. Secondly, darkening of some regions due to undesirable, unsharp masking effects is prevented. These undesirable effects are abnormal contrast augmentation and saturation of intensity levels of image which could be prevented by utilizing MUSM. As Figure 4 indicates, by comparing (4.d) and (4.c), the superiority of MUSM over USM is distinguished.

2.4 Adjusting the Directions for MUSM Filter

Building shadows specifies the building orientation in their one side. Most buildings have rectangular shape or quadrilateral shape; so, orientations of other side are parallel or perpendicular to the direction of shadow. To determine the orientation of motion blurring filter, first of all the shadows direction is computed using labeled binary map, obtained from original image. Then, coordination of pixels in each label is considered and the trend of each label is computed.

In this approach, Hough transform technique was introduced to obtain the orientation of each label and the directions utilized by the motion blurring function. Figure 4 shows the effect of MUSM on sharpening the image in different directions before and after threshold application. As figure 4 shows, best angle for making the dark building visible by MUSM is the perpendicular angle of shadow orientation. It is noticeable that the parameters such as $\frac{a}{T}$ and $\frac{b}{T}$ can be calculated by using the angle direction. The following formula indicates MUSM, in which the main format of Unsharp Masking is held:

$$G(u,v) = \sum_{-\infty}^{+\infty}\sum_{-\infty}^{+\infty}\left[\sum_0^{\tau} I(x-x_0, y-y_0)e^{-jux-jvy}\right]$$

$$= \sum_0^{\tau}\left[\sum_{x=-\infty}^{+\infty}\sum_{y=-\infty}^{+\infty} I(x-x_0, y-y_0)e^{-jux-jvy}\right]$$

$$= I(u,v).\sum_0^{x} e^{-jux_0(t)-jvy_0(t)} = I(u,v).H(u,v) \tag{15}$$

(15) applies the $G(u,v)$ in the (4). After the production of $\tilde{I}$, the Bayesian discriminator accomplishes detection of buildings, non-buildings and shadows.

2.5 Filtered-MUSM Method Assessment to Find Buildings

Elimination of some parts of non-buildings in remote sensing image can guarantee improvement of building extraction accuracy rate and error avoidance. These parts include roads and streets which are inaccurately classified as buildings. They should be deleted from the under-processing satellite images. Distribution and intensity of edges in building regions can be considered to define the space for investigation. Streets and roads have more dense edges along their sides as compared to buildings. However, the intensity of building edges is more than that of streets.

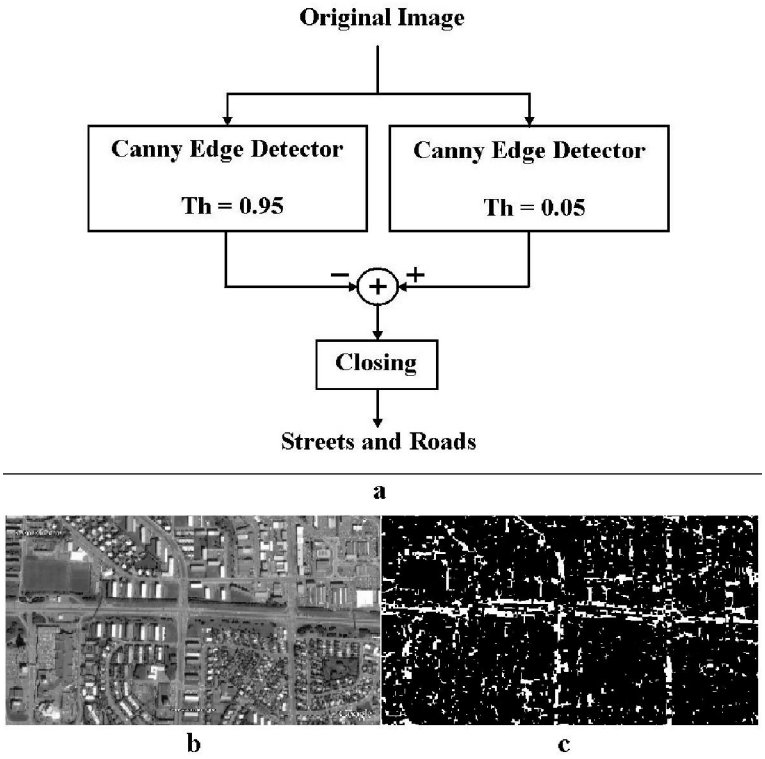

Figure 6. Detecting the streets and roads. The algorithm presents in 6.a, original image 6.b and the detected streets

As a result, the edges density and intensity will be two useful features to discriminate streets from buildings. Based on this idea, to eradicate the streets from the original image, an algorithm is given in a block diagram illustrated in figure 6. Thus, as figure 6 shows a filtered image which utilizes most of extracted roads and streets. For this purpose, firstly two different levels of threshold are employed to filter out very strong and very weak edges.

Afterwards, Closing operation is used to connect the edges and make integrated regions as detected streets. The detected parts of streets and roads were removed from the satellite image before applying the building extraction algorithm.

3. Experimental Results

In this section, application of proposed common methods to improve classification results is demonstrated. These approaches were applied to very high resolution remote sensing images from Reykjavik, Iceland. These images were obtained from Google Earth software. They have 3 channels (bands) including red, green and blue channels and their resolution is 1m. Although, panchromatic (4-band) satellite images are common for benchmarking such algorithms, availability of Google Earth images motivated us to develop and test the proposed algorithm by using 3-band Google earth images. Superiority and novelty of this paper in comparison with most of the current methods is its ability to extract building from Google Earth three bands (RGB) image. Three principal classes were considered in each case, namely:

1) Large buildings;
2) Houses (small buildings);
3) Shadows

Each image consists of urban area components including buildings, roads and open areas. The first step is the feature extraction by Laplacian and labeling operators. The second step is classification, using Bayesian discrimination function. This classification accuracy for the different pre-processing methods is compared to determine the global confidence in each pre-processing method. It is also compared with previous methods which previously presented by authors.

3.1 Results of the Testing Experiment

The first image, used to test (1024 × 716 pixels), is shown in Figure 1.1. To test the general

ability of the Bayesian classifier; some remote sensing images are used to benchmark the approach. The Bayesian training PDF function is obtained from marked images, namely training map. In the training map amounts of Laplacian, size, and intensity of each class was considered to evaluate the PDF function for each class. (Figure 4)

Appropriate levels of discriminated frequency, corresponding amounts of Laplacian, according to high frequency components of buildings and other low frequency levels of buildings were obtained using the training map. It is considerable that, the small buildings have high-frequency components since they have a grained texture on their edges. Furthermore, building roofs have smooth texture in satellite images.

The USM-based method outperformed the [19, 8] with regards to accuracies along Bayesian discriminator. Particularly, the most important goal of enhancement methods is improving Bayesian discriminator efficiency in building extraction. This objective is obtainable by adjusting frequency components of the remote sensing images. It makes the buildings more intensified rather than image background, discernable and improves local contrast of the remote sensing images. It minimizes drawback of unsharp mask filter which makes some of image regions disappear. For instance, image intensity reduction sometimes may happen in some section of image such as buildings, due to extra addition of dark edge causes the buildings to be eliminated.

3.2 Consequences of the Method without Preprocessing

The method without preprocessing step is introduced in the first part of the methodology. Bayesian discrimination function has demonstrated substantial results. However, it does not focus on adjusting high or low frequency restrictions. The γ_{SF} , λ values are 150, 0.5, respectively. The experimental results illustrate a complementary behavior between all methods, though the USM, MUSM, Filtered-MUSM accuracies are correspondingly improved.

Table. 1 Buildings Extraction Rate Based on First Method

Numbers of Satellite Images	Extracted Rate of Large Buildings	Extracted Rate of Small Buildings	False Negatives
57	5502	34253	1370

3.3 Results of Preprocessing Methods

The methods with no preprocessing step are utilized with no enhancement processes to improve the image contrast. Thus, the Bayesian discriminator results in error because some image components have similar level of intensity to the level of background intensity. The innovation of the proposed algorithm is usage of directional unsharp mask filter as preprocessing step for enhancing the image to be segmented. Adjusting the USM and MUSM parameters for enhancing the remote sensing image is a critical task which seriously affects the rate of building extraction.

3.4 USM-Family Method for Preprocessing

Using USM-family as filtering influences some features in the original image. Furthermore, remote sensing imagery has some intrinsic characteristics which make distinction with other images. Vegetations have low level of intensity in the red and blue channel spectrum. Therefore, the average amount of images in such regions is low. This phenomenon helps the classification methods to easily delete vegetations from building class. In this approach following conditions are considered to detect vegetations:

$$\begin{cases} R < 0.3 \\ B < 0.3 \\ G > 0.2 \end{cases} \quad (16.1)$$

$$\frac{(R+G+B)}{3} > 0.2 \quad (16.2)$$

Where R, G and B denote red, green and blue channels of the image, respectively. Last condition guarantees filtering out of the shadows from detected vegetations.

4. Synthetic Problems

4.1 Changing the Domain Description

A considerable synthetic problem is the Low pass filter or High pass filter behavior. They change domain description, especially in the building class. For example, when a low pass filter on the input images is applied, it reduces the classification rate of small buildings. On the other hand, the extraction of large buildings increases. This in fact is as a result of changes in image Laplacian and reverse relationship between size of buildings and frequency components.

4.2 Disappearance of Image Components

USM-family-based methods alter various parts of image intensity to boost the local contrast. Improvement of image contrast in regions with very low or very high intensity results in the disappearance or saturation of the level of intensity in these parts.

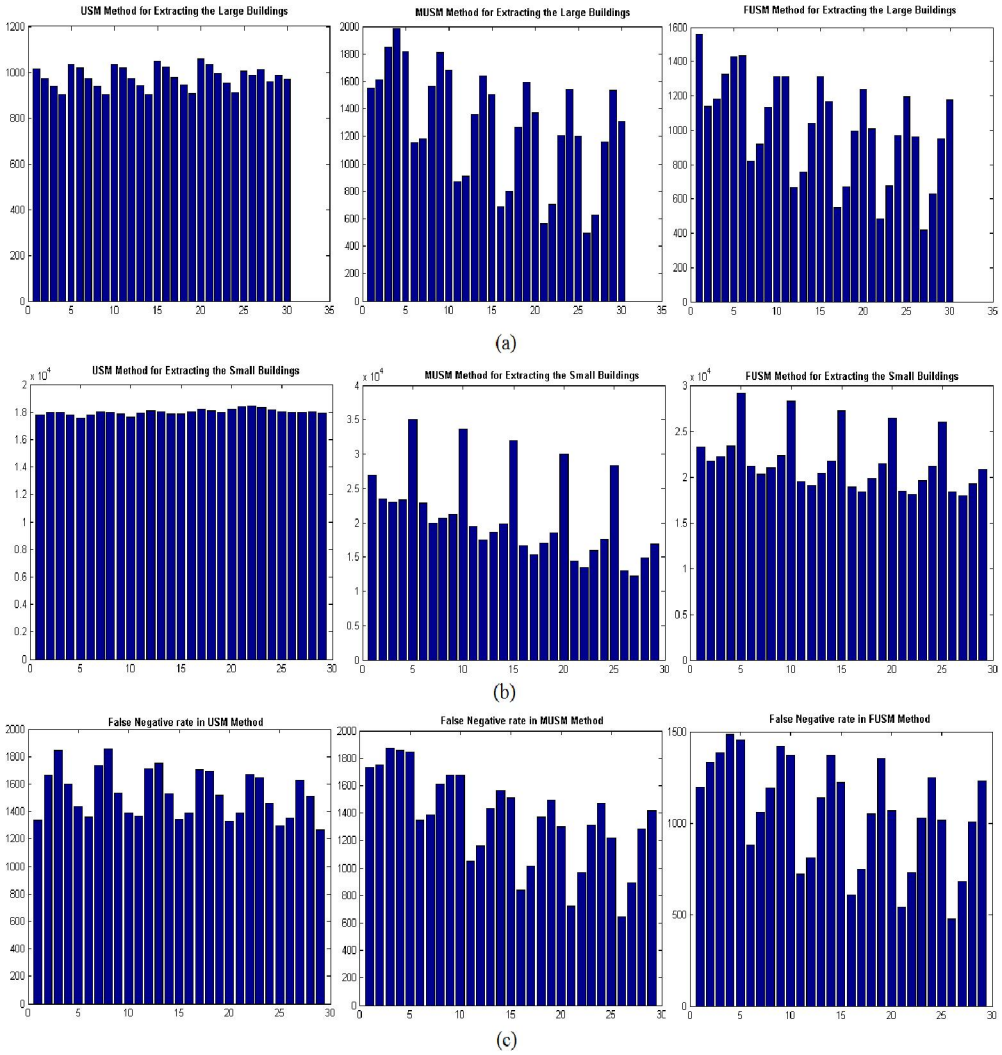

Figure. 7.a Current graph obtained by extraction of large buildings result of methods in variation of its parameters including amount and elongation; 7.b Current graph obtained by extraction of small buildings result of methods in variation of its parameters including amount and elongation 7.c The graphs show the rate of false negative in different methods.

Real Problems

The proposed methods were tested and showed following problems:

1) A number of buildings having the same intensity as the background can not be detected.

2) The color of a few roofs, affects classification accuracy.

3) Some fine particles in urban images increase classification errors. Moreover, these components can be erroneously classified as small buildings.

To overcome such problems, opening operator from morphological operation (MO) as filtering step along with the USM-family methods is used. Determining the size of the structure element (SE) is significant for designing morphological filters. Comparison is needed to determine SE size. Big sizes of SE remove small buildings while tiny sizes of SE can not remove the redundant particles of buildings class (non-building components). In this circumstance, these particles are classified as small buildings. As it was mentioned before, the SE size needs a trade-off between small and large sizes. Also, the SE sizes depend on the resolution of the remote sensing image. In this paper, the SE size in MO-filtering is equal to a 3-by-3 square matrix.

4.3 USM and MUSM Methods

The unsharp mask filter [USM] is a pre-processing method to increase the accuracy rate. Figure 5 and table 1 represent the accuracy rate of

small and large building extraction using the USM method in a remote sensing image set from Reykjavik, Iceland. As it is shown in figure 9, amount of small and large buildings are closer to real numbers of buildings than the non-preprocessing method. In other words, the number of buildings that are not detected using the method with preprocessing step is lower than that of the other method. [MUSM] method improves the extraction rate of buildings. Figure 9 points out the rate of correctness in small and large building detection when the MUSM method is utilized. The correlations between extracted small and large buildings compared with the last methods are clearly depicted in figure 7 and detailed in appendix A. Entirely MUSM and, USM method have modified the rate of accuracy, respectively.

4.4 Filtered MUSM Methods

Subsequent to pervious section about the MUSM method, there are several false positive results, which are depicted in MUSM results. It reduces the rate of USM-family accuracy because some of roads and streets are classified as buildings in error. As a remedy, a filter based on Canny edge detection and Morphological operation is utilized to extract roads and street parts and delete them from the image. It diminishes false positive and increases the rate of correct detection. The threshold values for canny edge detectors are 0.05 and 0.95. The structure element for Closing operation is a 8-by-8 square. Although, it is demonstrated in Table 1 that the rate of MUSM building extraction is more than Filtered-MUSM method, Filtered-MUSM reduces the false positives. It helps the USM-family to identify buildings more efficiently. The results of these additional experiments reveal the necessity of parameter adjustment of the mentioned methods. In table 1, Results are depicted per each method according to changing various parameters. Generally, results indicate the improvement of accuracies after parameter adjustment.

5. Conclusion

In this novel paper, a fully automated method for building extraction from very high resolution satellite images is presented. Firstly USM-family methods for preprocessing step are presented. The USM-family intends to improve the image contrast and modify the image frequency components. Then, the Bayesian discriminator is used to take out buildings from the images. Finally, the USM-family method accuracies are boosted by a special filter based on canny edge detector and morphological operations. Experiments reveal promising results and the efficiency of the proposed approach, in the task of building extraction.

Acknowledgements:

The authors would like to thank the Google Earth and Satellite Imaging Corporation for providing satellite images for research purposes. Authors are grateful to Dr. Alireza AhmadyFard and the Department of Electrical and Robotic Engineering, Shahrood University of Technology in Iran for supporting to carry out this work.

Corresponding Author:
Bardia Yousefi
Department of Electrical and Robotic Engineering, Shahrood University of Technology, Shahrood, IRAN. E-mail: bardia.yousefi@ieee.org

References

1. Bardossy A., Samaniego, L. 2002. Fuzzy rule-based classification of remotely sensed imagery, IEEE Trans. Geosci. Remote Sensing. 35(2): 362–374.
2. Bruzzone, L., Carlin, L. Melgani, F. (2004) .A Multilevel Hierarchical Approach to Classification of High Spatial Resolution Images with Support Vector Machines. IEEE International conference held at Anchorage, AK, USA: IGARSS pp.20-24.
3. Chijioke G. Eze (2009). The role of satellite remote sensing data and GIS in population census and management in Nigeria: A case study of an enumeration area in Enugu, Nigeria. Scientific Research and Essay, 4 (8): 763-672.
4. Couloigner I., Ranchin, T.2000 .Mapping of urban areas: A multi-resolution modeling approach for semi-automatic extraction of streets, Photogramm. Eng. Remote Sens., 66 (7): 867–874.
5. Davis C H, Wang X (2002). Urban Land Cover Classification from High Resolution Multi-Spectral IKONOS Imagery. International Geoscience and Remote Sensing Symposium, Proceedings of an international conference held at Toronto, Canada, IGARSS 2002: pp.24–28.
6. Dell'Acqua F, Gamba P., 2001. Detection of urban structures in SAR images by robust fuzzy clustering algorithms: The example of street tracking, IEEE Trans. Geosci. Remote Sensing, 39(1): 2287–2297.
7. M. Fauvel, J. Chanussot and J. A. Benediktsson (2005). Fusion of Methods for the Classification of Remote Sensing Images from Urban Areas. International Geoscience and Remote Sensing Symposium, Proceedings of an international conference held at Seoul, Korea: IGARSS 2005, pp. 2819 - 2822.
8. Fauvel M., Chanussot, J., Atli Be, J.2006. Classification of Remote Sensing Images from Urban Areas Using a Fuzzy Possibilistic Model, IEEE Geosci. Remote Sensing Letters,3(1):40-44.
9. Jenson J R(1996). Introductory Digital Image Processing: A Remote Sensing Perspective, 2nd ed. Upper Saddle River, NJ: Prentice-Hall.
10. Kressler, F.P. Bauer, T.B. Steinnocher, K.T. 2002. Object-oriented perparcel land use classification of very high resolution image. Remote Sensing and Data Fusion over Urban Areas, Proceedings of an international Workshop held at Rome, Italy, IEEE/ISPRS: pp. 164–167.
11. Farid Melgani, Bakir A. R. Al Hashemy, and Saleem M. R. Tahar. 2000. An explicit fuzzy supervised classification

method for multispectral remote sensing images, IEEE Trans. Geosci. Remote Sensing, 38(1): 287–295.
12. Nisanci R(2010). GIS based fire analysis and production of fire-risk maps: The Trabzon experience. Scientific Research and Essays, 5(9): 970-977.
13. Pesaresi. M. 1999. Textural classification of very high-resolution satellite imagery: Empirical estimation of the interaction between window size and detection accuracy in urban environment, Proceedings of the 1999 International Conference on Image Processing held at Kobe, Japan, ICIP 99: pp.114–118.
14. Pesaresi M., Benediktsson, J. A. 2001. A new approach for the morphological segmentation of high-resolution satellite imagery. IEEE Trans. Geosci. Remote Sensing, 39(2): 309–320.
15. Shackelford A K, Davis C H. 2002. A fuzzy classification approach for high-resolution multispectral data over urban areas. In: International Geoscience and Remote Sensing Symposium, Proceedings of an international conference held at Toronto, Canada, IGARSS 2002: pp.1621–1623.
16. Shandiz H., Mirhassani, M. S., Yousefi, B.2008. Hierarchical Method for Building Extraction in Urban Area Images using UnSharp Masking [USM] and Bayesian classifier. In: 15th International Conference on Systems, Signals and Image Processing, Proceedings of an international conference held at Bratislava, Slovak Republic, IWSSIP'08: pp.193 – 196.
17. Steger, C.1998. An unbiased detector of curvilinear structures, IEEE Trans. Pattern Anal. Machine Intel., 20(2): 113–125.
18. Tatem A. J., Lewis, H. G., Atkinson, P. M. ,and Nixon M. S. 2001. Super-resolution mapping of urban scenes from IKONOS imagery using a Hopfield neural network. In: International Geoscience and Remote Sensing Symposium, Proceedings of an international conference held at Sydney Australia, IGARSS 2001: pp.3203–3205.
19. Yousefi B., Mirhassani, S.M., Marvi H.2007. Classification of remote sensing images from urban areas using Laplacian image and Bayesian theory. Proceedings of an international conference of SPIE held at Lausanne Switzerland, SPIE 2007: pp. 6718:1-9.
20. Ebrahimi,E., Mollazade, K, Arefi, A.2011. Detection of Greening in Potatoes using Image Processing Techniques. Journal of American Science. 7(3):243-247.
21. Elyasi, A., Ganjdanesh, Y., Kangarloo, K., Hossini M. Level set segmentation method in cancer's cells images. Journal of American Science 2011; 7(2):196-204.
22. Mohammadi Torkashvand, A., The Preparation of Paddy Map by Digital Numbers of IRS images and GIS. Journal of American Science 2011;7(1):382-385.
23. Elyasi, A., Ganjdanesh, Y., Kangarloo, K., Hossini, M., and Esfandyari, M.2011. Level set segmentation method in cancer's cells images. Journal of American Science.7(2):196-204.

24/01/2012

Appendix 1

Table. 2 Building Extraction Rate Based on USM, MUSM, Filtered-MUSM Methods and classification in terms of accuracies.

		USM			MUSM			Filtered-MUSM		
Amount	Elongation	Extracting Rate of Large Buildings	Extracting Rate of Small Buildings	False Negatives	Extracting Rate of Large Buildings	Extracting Rate of Small Buildings	False Negatives	Extracted Rate of Large Buildings	Extracted Rate of Small Buildings	False Negatives
2	5	1034	17538	1438	1863	36020	1881	1562	29610	1618
2.7	10	1017	17818	1336	1552	26929	1732	1140	23285	1196
3.4	15	972	18010	1663	1614	23395	1749	1180	21682	1331
4.1	20	940	17977	1843	1852	22939	1876	1326	22261	1382
4.8	25	902	17829	1602	1985	23289	1858	1428	23368	1484
5.5	5	1033	17556	1438	1817	35011	1846	1436	29204	1455
2	10	1018	17821	1358	1154	22888	1350	822	21155	878
2.7	15	973	18032	1733	1184	19912	1389	918	20301	1060
3.4	20	939	17998	1856	1562	20588	1612	1135	20968	1191
4.1	25	903	17839	1537	1809	21244	1674	1311	22366	1420
4.8	5	1035	17659	1386	1684	33592	1675	1314	28265	1370
5.5	10	1018	17896	1366	868	19507	1052	667	19516	723
2	15	974	18082	1708	908	17472	1163	755	19095	811
2.7	20	942	18030	1750	1360	18639	1436	1039	20418	1137
3.4	25	903	17869	1527	1641	19802	1564	1314	21730	1370
4.1	5	1048	17862	1343	1505	31952	1510	1166	27228	1222
4.8	10	1024	18048	1388	685	16684	838	551	18866	607
5.5	15	977	18200	1706	797	15375	1013	673	18415	746
2	20	945	18128	1692	1266	17050	1373	995	19849	1051
2.7	25	907	18010	1520	1594	18521	1493	1239	21481	1355
3.4	5	1057	18224	1333	1370	30032	1304	1010	26465	1066
4.1	10	1034	18401	1386	566	14498	723	485	18489	541
4.8	15	994	18460	1669	702	13525	968	675	18127	731
5.5	20	952	18311	1647	1206	15914	1312	971	19589	1027
2	25	909	18180	1457	1542	17617	1471	1193	21183	1249
2.7	5	1004	18058	1298	1199	28353	1218	960	25977	1016
3.4	10	986	17963	1353	494	13003	646	419	18391	475
4.1	15	1014	17986	1630	628	12204	891	627	17961	683
4.8	20	958	18065	1510	1161	14901	1286	952	19268	1008
5.5	25	987	17942	1267	1536	16880	1420	1176	20866	1232